# CASE STUDIES TO ILLUSTRATE THE ROTORCRAFT CERTIFICATION BY SIMULATION PROCESS; CS 29/27 LOW-SPEED CONTROLLABILITY

Stefan van 't Hoff, Royal Netherlands Aerospace Centre, NLR, Amsterdam, The Netherlands
Mark White, University of Liverpool, Liverpool, UK
Christopher Dadswell, University of Liverpool, UK
Linghai Lu, Cranfield University, Cranfield, United Kingdom
Gareth Padfield, University of Liverpool, Liverpool, UK
Giuseppe Quaranta, Politecnico di Milano, Milano, Italy
Philipp Podzus, German Aerospace Centre, DLR, Braunschweig, Germany

## Abstract

This paper is one of a set presented at the 49th European Rotorcraft Forum discussing results from the EU Clean Sky 2 project, Rotorcraft Certification by Simulation (RoCS). The process developed by the RoCS team provides guidance on the use of flight simulation in certification and features four case studies that illustrate aspects of the process using flight simulation models and flight test data provided by Leonardo Helicopters. This paper presents the case study for the low-speed controllability requirements from the relevant certification paragraphs in the EASA Certification Specifications CS-27 and CS-29. Following an introduction of the related specifications, and the motivation behind seeking compliance supported by simulation, the various phases of the RCbS process are explored in more detail. The intent is to exercise aspects of the RoCS guidance in a practical application to investigate the implementation, and the strengths and limitations, given real-world constraints. Emphasis is placed on the Validation & Verification as well as the Credibility Assessment, taking into account test and simulation uncertainties. Results from piloted simulation trials are included to illustrate possible flight simulator fidelity assessment methods.

## NOTATION

Symbols

| | |
|---|---|
| $\delta_{inp}$ | Error due to input parameters |
| $\delta_{model}$ | Simulation model error |
| $\delta_{num}$ | Numerical solution error |
| $\delta_{val}$ | Validation error |
| $\ddot{\theta}$ | Simulation model pitch acceleration |
| $\ddot{\theta}_s$ | Motion platform acceleration |
| $\omega$ | Frequency, rad/s |
| $\omega_{hpx,y,z}$ | 2nd order high-pass, surge, sway and heave motion filter break-frequency |
| $\omega_{hp\phi,\theta\psi}$ | 2nd order high-pass, roll, pitch and yaw motion filter break-frequency |
| $k_{x,y,z}$ | Surge, sway, heave high-pass motion filter gain |
| $k_{\phi,\theta,\psi}$ | Roll, pitch, yaw high-pass motion filter gain |
| $n_{TF}$ | Number of transfer functions |
| $n_\omega$ | Number of frequency points |

| | |
|---|---|
| $J_{ave}$ | Frequency response integrated cost function |
| $R$ | Referent (measurement) value |
| $S$ | Simulation prediction |
| $T$ | Transfer function |
| σ | Density ratio |
| $u_{inp}$ | Input parameter uncertainty |
| $u_{num}$ | Numerical solution uncertainty |
| $u_R$ | Referent uncertainty |
| $u_{val}$ | Validation uncertainty |
| $W_\gamma$ | Frequency response coherence weight |
| $W_g$ | Frequency response magnitude weight |
| $W_p$ | Frequency response phase weight |
| XA,XB, XC,XP | Pilot controls, lateral cyclic, longitudinal cyclic, collective, pedal |

Acronyms

| | |
|---|---|
| AC | Advisory Circular |
| ACR | Applicable Certification Requirements |
| ADS-33 | Aeronautical Design Standard-33 |
| CS | Certification Specification |
| DoE | Domain of Extrapolation |
| DoP | Domain of Prediction |
| DoR | Domain of Reality |
| DoV | Domain of Validation |
| EASA | European Union Aviation Safety Agency |
| EP | Evaluation Pilot |
| ERF | European Rotorcraft Forum |
| FAA | Federal Aviation Administration |
| FS | Flight Simulator |
| FSM | Flight Simulation Model |
| FTM | Flight Test Manoeuvre |
| FTMS | Flight Test Measurement System |
| HQR | Handling Qualities Rating |
| IGE | In Ground Effect |
| IPC | Influence, Predictability, Credibility |
| MTE | Mission Task Element |
| OGE | Out of Ground Effect |
| PCE | Pace Car Equivalent |

| | |
|---|---|
| RoCS | Rotorcraft Certification by Simulation |
| RCbS | Rotorcraft Certification by Simulation |
| SFR | Simulation Fidelity Rating |
| V&V | Validation & Verification |
| VRS | Vortex Ring State |
| XWH | Cross-Wind Hover |

## 1. INTRODUCTION

A newly developed aircraft must be certified before entering service by demonstrating compliance with the safety requirements set by aviation certification authorities. Both the structure of the certification process and the means to demonstrate compliance with the regulations must be agreed between the manufacturer, or more generally the applicant, and the authority. The compliance demonstration is usually performed through flight and ground tests that are typically the lengthiest and most expensive part of the development process. Compliance flight tests can pose safety concerns, such as those related to flight control system or engine failures. To optimise the scope of flight test activities through reducing the cost and time required for the tests, whilst lowering the potential risk, advanced analysis-based methods of compliance, such as flight simulation, are being explored. As an exemplar, Leonardo Helicopters used simulation in the certification of the engine-off landings for the AW189 (Ref. 1), and tail rotor loss of effectiveness for the AW169 (Ref. 2). Both European Union Aviation Safety Agency's (EASA's) CS-27 and CS-29 Subpart B define the term "*analysis-based*" methods of compliance as "*calculations*" in the clause of "*tests upon a rotorcraft of the type for which certification is requested, or by calculations based on, and equal in accuracy to, the results of testing*" (Refs. 3, 4). Federal Aviation Administration (FAA) Advisory Circular AC-29.21(a) states "*calculation*" includes flight simulation (Ref. 5). FAA's AC 25-7D §3.1.2.6 defines the general principles under which flight simulation may be proposed as an acceptable alternative to flight testing for large aeroplanes (Ref. 6). With the increase in fidelity of physics-based rotorcraft flight simulation models, it is foreseeable that the usage of flight simulation to replace or augment flight testing through a virtual-engineering process will become more dominant, as the industry pursues efficiency, low cost, increased safety, and low energy consumption (Ref. 7). The team of the European CleanSky2 funded project, Rotorcraft Certification by Simulation

(RoCS), has the aim to explore the possibilities, limitations, and guidelines for best practices for the application of flight simulation to demonstrate compliance with the airworthiness regulations related to helicopters and tiltrotors (Ref. 8).

Under the framework of the RoCS project, preliminary Guidance for the application of (rotorcraft) flight modelling and simulation has been developed in support of certification for compliance with standards CS-27/29, PART B (Flight) and other flight-related aspects (e.g. CS-29, Appendix B, Airworthiness Criteria for Helicopter Instrument Flight) (Refs. 9, 10, 11). The Guidance follows a requirements-based approach and is presented in the form of a structured process for Rotorcraft Certification by Simulation (RCbS)[1]. The process starts with the selection of 'applicable certification requirements' (ACRs) for the application of RCbS, with judgements on a matrix of factors of Influence (how the RCbS process will be applied), Predictability (the extent of interpolation or extrapolation), and Credibility (the level of confidence in results). Case studies drawn from selected ACRs have been conducted to demonstrate the efficacy of aspects of the process, and include example fidelity metrics and tolerances for fidelity sufficiency and credibility analysis.

This paper presents the results from the case study on CS 27/29.143(c), 'controllability and manoeuvrability in winds up to 17 knots', to illustrate the application of the Guidance. Section 2 provides an overview of the RCbS process, parts of which will be elaborated on herein. The low-speed controllability ACR and the related motivation an applicant may have to explore RCbS are discussed in Section 3. The subsequent Sections 4 through 7 explore the various Phases of the RCbS process in more detail, including results from preliminary piloted simulation trials. Finally, tentative conclusions and recommendations for ongoing work are offered in Section 8.
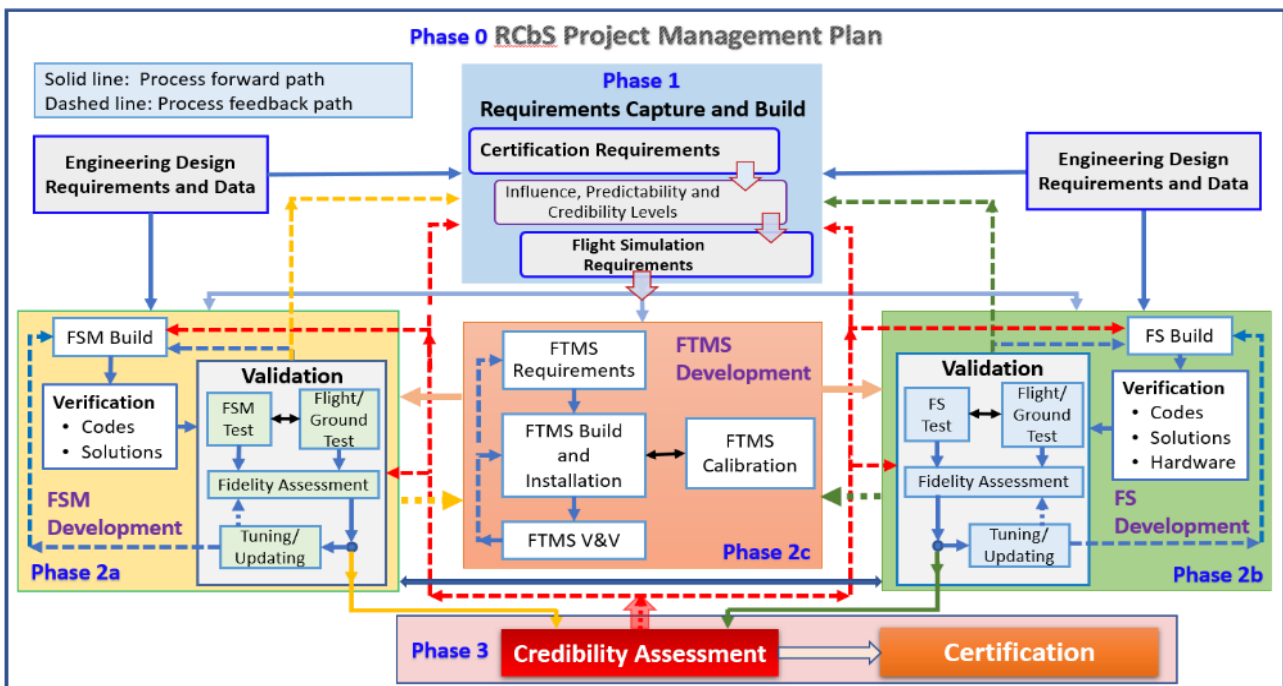


Figure 1: The RCbS process summarised as a flow diagram (Refs. 9-11).

---

[1] To distinguish between the two acronyms, RCbS refers to the process developed by the RoCS 'project' team.

## 2. OVERVIEW OF THE RCBS PROCESS

The Guidance for the RCbS process is organised into three, serial but iterative, phases, as shown in Figure 1 and expanded on in Refs. 9 and 10.

1) Phase 1; Requirements Capture and Build
2) Phase 2; Developments of Flight Simulation Model (FSM, 2a), Flight Simulator (FS, 2b) and Flight Test Measurement System (FTMS, 2c)
3) Phase 3; Credibility Assessment and Certification

The activities in these three phases are undertaken within a governance-framework defined in the Project Management Plan and created in Phase 0 of the RCbS process.

The application of RCbS is contained within different domains as illustrated in Figure 2. In summary, the domains are:

a) The domain of physical reality (DoR) is the domain within which the laws of physics being used are considered to be adequately represented in the flight model and flight simulator.
b) The domain of prediction (DoP) is the domain within which it is the intention to predict the behaviour of the aircraft and its components and to use these predictions to support certification at the defined I-P Levels.
c) The domain of validation (DoV) is the domain within which test data are used to validate the flight simulation. Interpolation is used in the DoV to predict behaviour between validation points.
d) The domain of extrapolation (DoE) is the domain within which extrapolations of predictions are made to achieve certification at defined Influence Levels for an ACR.

Phase 1 contains subtasks for a given ACR, selecting the appropriate Influence and Predictability (I-P) levels, defining the simulation types and critical features, and assembling their detailed requirements. The RCbS Guidelines (Ref. 11) use the concepts of Influence, Predictability and Credibility (IPC) levels to convey meaning to the underlying consequences of the application of RCbS, in terms of safety and efficiency in the certification campaign. The IPC Levels inform the FSM and FS requirements capture and build phases of the RCbS process.
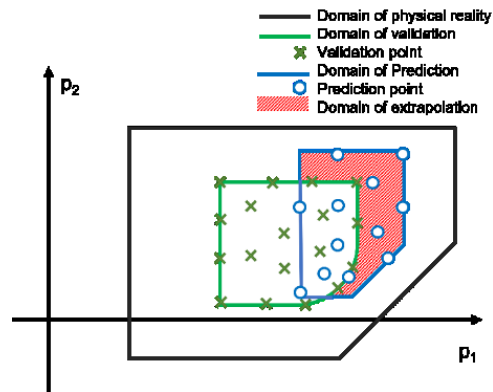


Figure 2: The domains in the RCbS process (Ref. 11).

Figure 3 illustrates an example of how the I-P matrix might be configured, showing the four forms of Influence and Predictability (i.e., 16 possible combinations). IPC levels towards the bottom right of the table are generally associated with a higher degree of uncertainty in the predictions and will require a more rigorous approach to quantifying that uncertainty. In practice, an applicant may go through multiple stages of the IPC table during the development and certification process. In fact, in case of Influence level I1 (De-risking), certification compliance demonstration is performed solely through flight testing, and involvement of the certification authority in the simulation phase is not a prerequisite. In Figure 3 IPC level I4P3 is highlighted to indicate the example case considered in this paper.

| RCbS ACR | Influence Levels | Predictability Levels | | | |
|---|---|---|---|---|---|
| | | Full Interpolation in DoV (P1) | Extensive interpolation in DoV / Limited extrapolation in DoE (P2) | Interpolation in DoV / Extensive extrapolation in DoE (P3) | Full extrapolation in DoE (P4) |
| ACR 27.143 (Controllability and Manoeuvrability) 1. Control margins for low-speed manoeuvring in winds | De-risking (I1) | | | | |
| | Critical Point Analysis (I2) | | | | |
| | Partial credit (I3) | | | | |
| | Full credit (I4) | | | | |

Figure 3: Example selection of the Influence and Predictability levels in the RCbS process.

This paper aims to provide an example implementation of the RCbS process for the low-speed controllability ACR considering the various RCbS phases in a hypothetical certification scenario described in the

following section. In practice, the most suitable approach to the RCbS process will be dependent on the applicant and the circumstances. As will become apparent in subsequent sections, the RCbS process is a systematic and rigorous one, and careful deliberation will always required before deciding on the best approach to take in a given situation.

## 3. ACR AND RCbS MOTIVATION

CS-29.143(c) states:

*Wind velocities from zero to at least 31 km/h (17 knots), from all azimuths, must be established in which the rotorcraft can be operated without loss of control on or near the ground in any manoeuvre appropriate to the type (such as crosswind take-offs, sideward flight, and rearward flight), with:*

*(1) Critical weight;*

*(2) Critical centre of gravity;*

*(3) Critical rotor rpm; and*

*(4) Altitude, from standard sea-level conditions to the maximum take-off and landing altitude capability of the rotorcraft.*

Although the requirements relate to 'any manoeuvre appropriate to the type', the focus in this paper will be on hover in cross-wind conditions. It must be demonstrated that a hover in wind from any direction can be established, maintained and transitioned to/from without loss of control. The guidance in AC 29-2C further states that it must be demonstrated that sufficient control power should be available to permit a clearly recognisable yaw response with wind from the critical azimuth. The applicant must then define the weight, altitude and temperature limitations within which the requirements are met.

Flight testing for compliance demonstration for the low-speed controllability requirements is traditionally performed in calm winds using a pace car (or equivalent) over a runway for visual reference. Although there is some discussion as to whether the conditions in this testing approach are truly equivalent to operational cross-wind hover tasks, this method is often preferred over hover testing considering the difficulties in obtaining the desired steady wind conditions. In either case, the demonstration of control power, or the ability to affect a recognisable yaw response, typically involves demonstrating transient heading changes of ±5 degrees from the critical direction and back. The term 'critical conditions is used to include

any combination of wind magnitude and direction where control margins or handling qualities effects limit controllability.

In traditional development and certification, the flight test effort required to characterise the controllability of the aircraft, and ultimately demonstrate compliance to the certification requirements, is extensive. In particular, the requirement to demonstrate compliance up to the maximum take-off and landing altitude capability implies a time-consuming and costly relocation to high-altitude test sites. Although the high-altitude test activities are combined with various other test objectives, and cannot be avoided entirely, reduction in the time spent on-site and minimisation of the likelihood of encountering unexpected design limitations are considered highly desirable. Moreover, extensive simulation efforts in advance of flight testing, either offline or in a flight simulator, limit the risks associated with any remaining flight testing. Despite the low-speed nature, the in-ground-effect testing for this requirement is performed partly inside or close to the limits of the height-velocity diagram and is, therefore, inherently high-risk. The risk of loss of control at the pedal margin limits is another motivator for the use of simulation to reduce the safety risks in the context of this ACR.

With these objectives in mind, what remains is to develop and demonstrate the ability to predict the behaviour of the aircraft in the relevant flight conditions with sufficient fidelity and credibility at a cost, in time and effort, that is not prohibitive. The RCbS process as outlined in the RoCS guidelines is but a first step in that direction.

## 4. PHASE 1: REQUIREMENTS CAPTURE AND BUILD

### 4.1 Influence & Predictability

In RCbS Phase 1, the applicant and authority must agree on the extent to which simulation will be relied upon in the finding of compliance. This includes an expectation as to how far the predictions may be extended beyond the validation flight test data in whatever extrapolation dimension may be applicable. It is assumed for this case study that the applicant desires to use simulation to determine the critical wind speeds and directions and associated take-off weight limitations, accounting for the control power and controllability requirements for IGE and OGE hover. Flight testing for low-speed controllability at the maximum altitude capability is not intended to be

performed. Thus, the influence level as defined in the RoCS guidelines, and discussed in section 2, corresponds to I4, Full Credit. The simulations are planned for conditions up to the envisioned maximum take-off and landing altitude at 12,000 ft density altitude. Initial flight testing for demonstration and simulation validation is planned to be performed up to 7,000 ft. AC 29-2C allows altitude extrapolation of maximum ±2,000 ft for IGE controllability assessment, putting this use case clearly in the P3, "Extensive extrapolation in DoE", predictability level. However, if limited high-altitude flight testing is later performed, e.g., to provide evidence for the absence of limitations due to exhaust gas re-ingestion and compressor surge, such testing would ultimately provide additional validation data. This data would then significantly reduce the extent of the extrapolation for an iteration on the validation and simulation predictions if needed.

## 4.2 Initial FSM & FS Requirements

Having established the conditions and objectives for the use of simulation as part of the certification plan, the next step is to establish, as far as can be foreseen in advance, the requirements that the FSM, the FS and the validation flight test data must meet. The prediction, through simulation, of the available control power at the critical azimuth, typically with wind from around 90 degrees, may be performed offline (although piloted simulation may serve to tease out FSM anomalies). A controllability assessment aimed at limitations due to a deterioration in handling qualities, typically at azimuths characterised by significant vortex wake interactions, requires piloted simulation in a suitable FS, although offline predictions of stability and response can be used to guide the FS trials. The applicant, therefore, plans to employ both offline desktop and piloted simulations (with the FS running either on the same or a derived and cross-correlated real-time FSM).

The following high-level FSM characteristics are anticipated by the applicant to be required at minimum to achieve acceptable credibility:

- Physics-based modelling (extrapolation)
- Rigid blade element main & tail rotor
- Rotor wake interference effects
- Dynamic Vortex Ring State model (tail rotor)
- Ground effect model
- Engine deck: installed minimum spec. power
- Rotor speed governor dynamics
- Uniform steady atmospheric wind model

One of the key difficulties for this particular application is the modelling of the wake interactions between the rotors, fuselage, empennage and the ground. With contemporary computing power, real-time piloted simulations will require some form of reduced order modelling, e.g., in the form of data maps. Vortex Ring State (VRS) is mentioned here specifically because typical momentum theory modelling of VRS is aimed primarily at avoiding a singularity or discontinuity in the solution of the inflow model, but does not capture the low-frequency unsteady nature, or the time lag associated with the development of the rotor inflow state (Refs. 12-14).

Prior to establishing draft requirements for the flight simulation, the applicant must define the manner in which the trials are to be performed. In the case of the low-speed controllability ACR, validation of the Handling Qualities Ratings (HQRs) awarded in the simulator will require a scenario, or Flight Test Manoeuvre (FTM), that is comparable in terms of task and cueing environment to the flight test procedure. Thus, at least the simulator trials performed for validation purposes will be conducted in a zero-wind pace car type of set-up (see Appendix A for proposed FTM). However, the FS environment offers the opportunity to develop an FTM that is more comparable to the operational tasks associated with the ACR. Hence, it is assumed in this case study that the applicant proposes a 'hover turn in wind' FTM for the predictions at altitude (see Appendix B).

The following high-level flight simulator characteristics are anticipated by the applicant in this scenario to be required at a minimum to achieve sufficient perceived simulation fidelity:

- Inceptors with appropriate control loading
- Vestibular motion cueing: non-essential
- Visual cueing environment: sufficient to perform task without objectional pilot adaptation
- Vibration and audio cues: non-essential
- Generic instruments

The visual cueing environment is influenced by many characteristics of the FS set-up, including the field of view, ground textures and contrast, and the visual content (i.e. objects). In the case of the proposed 'hover turn in wind' FTM, artificial cues similar to those included in the precision hover Mission Task Element (MTE), defined in ADS-33E-PRF (Ref. 15), are required, where the definition of adequate and desired performance needs to be related to typical civil

operations in wind. Although standardised to an extent (e.g. in terms of artificial visual cues), the sufficiency of the cueing environment for the specific ACR should be investigated early in the RCbS process through exploratory trials in the FS. The cockpit instruments do not need to be exact hardware or software replicas of the production aircraft, but it is considered essential that the scanning pattern and sequence match those observed in flight (which can be demonstrated, e.g., through eye tracking measurements).

Vestibular motion cueing, although considered by the applicant to be non-essential in principle, can be useful in providing early cueing of, e.g., lateral drift, thereby improving task performance and reducing pilot adaptation. The absence of such cueing may be considered conservative, but care must be taken to ensure that the pilot adaptation does not impede the handling qualities evaluation. To avoid adverse vestibular motion cueing, it is essential that the motion system is properly calibrated for the specific manoeuvre being investigated.

Beyond establishing the objectives for the use of flight simulation and defining an initial set of simulation requirements, the applicant must put forth a plan at the end of Phase 1 that outlines the approach to, and data requirements for, Verification & Validation (V&V), Fidelity Assessment, Credibility Assessment, and the final compliance demonstration. These elements will be discussed in the following sections.

## 5. PHASE 2A: FSM BUILD AND DEVELOPMENT

The RoCS project was provided with flight test data and a FLIGHTLAB FSM of the AW109 Trekker by Leonardo Helicopter Division (LHD) with which to exercise aspects of the RCbS process. Flight data for trims, stability and response assessment were provided to the RoCS team for a range of test conditions, prior to any FSM analysis. Note that in the formal RCbS process, the flight test data would be gathered in Phase 2, in conjunction with the development of the FSM and FS and following the development (incl. V&V) of the FTMS.

### 5.1 FSM Build

In accordance with the RCbS process, the FSM development phase should follow a structured approach with basic V&V building up from component to aircraft level. Physics-based modelling is considered an essential prerequisite to support extrapolation, as is the situation in this case study. The baseline FSM that formed the starting point for the RoCS activities was developed by LHD and was validated for up-and-away flight conditions, but not for low-speed conditions in proximity to the ground. The continued FSM development within RoCS was jointly aimed at the simulation of low-speed controllability, dynamic stability, and Category A take-off procedures (Ref. 16).

The baseline FSM features a rigid articulated blade-element main rotor. The tail rotor is modelled as a disk-type collective-only rotor (Bailey model), with aerodynamic properties originally tuned to level-flight pedal-to-yaw frequency response characteristics. The main rotor induced velocities are computed with a Peters-He three-state inflow model, along with a source-image ground-effect model. The rotor aerofoil data are available in the form of table lookup of the aerodynamic coefficients $C_l$, $C_d$ and $C_m$ as functions of angle of attack and Mach number. The blade airloads are computed in a quasi-unsteady fashion including unsteady circulatory effects from thin airfoil theory. The fuselage aerodynamic loads are computed at, and applied to, a single computational point. The fuselage and empennage force and moment coefficients are available as functions of angles of attack and sideslip, derived from model-scale wind tunnel test data.

The baseline FSM displayed several fidelity deficiencies in hover and low-speed flight (incl. hover in crosswind). The prediction of control positions and attitudes in trim, critical for this ACR, did not meet typical fidelity standards, e.g., those of CS-FSTD(H), Ref. 17. In fact, predicting the interactional aerodynamic effects that occur on conventional main-tail rotor helicopter configurations in hover with winds from all directions is likely beyond the capability of current state-of-the-art (real-time) simulation methods. Nevertheless, an attempt was made to improve the fidelity of the FSM to enable a sensible exploration of the RCbS process.

As stated, the main shortcomings of the physical modelling lay in the approximation of the interactional aerodynamics. The typical fuselage interference modelling in FLIGHTLAB (Ref. 18) uses a lookup table that provides the aerodynamic force coefficients as functions of the angles of attack and sideslip. In the baseline FSM, a single Aerodynamic Computational Point (ACP) was used, disregarding the distribution of interference velocities and cross-sectional area of the fuselage. In an attempt to account for these effects empirically, multiple ACPs have been

defined by a set of locations along the length of the fuselage with a weighting defined by the local fuselage volume or projected area. The interference velocity vector used for table look-up is obtained through weighted averaging across the ACPs. The one-way look-up table interference modelling relies on the validity of the aerodynamic data table and the main rotor wake model. In this case, the data table was compiled by LHD from multiple wind tunnel experiments of different airframe configurations. The composite nature of the data raises some concerns considering the applicable range of incidence angles, but addressing these was beyond the scope of the project. Instead, aiming also to improve rotor performance modelling itself, effort was put into increasing the fidelity of the finite-state main rotor inflow model through ΔL-matrix augmentation derived from a Viscous Vortex Particle Method (VVPM) model based on the method proposed in Refs. 19 and 20. It was found, however, that the number of inflow states required to approximate the VVPM inflow distribution remained prohibitive for real-time piloted application and the approach was abandoned.

Another crucial aspect of the FSM for the low-speed controllability ACR is the fidelity of the tail rotor model. The pedal control authority and the handling qualities in the yaw axis are heavily influenced by main rotor wake - tail rotor interference and tail rotor VRS conditions. The baseline disk tail rotor modelling can capture such effects only with a low level of fidelity. Part of the offline analyses and FS testing was, therefore, performed with a blade element tail rotor model with finite-state inflow. The offline pedal trim results improved marginally in comparison to flight test in winds from around 11 o'clock, but in the conditions tested in the FS the pilot did not report a significant influence on the perceived handling qualities, although the findings on this topic are not conclusive. Note, however, that for the following sections the precise level of fidelity achieved is not critical to the objective of illustrating the RCbS process.

## 5.2 FSM Verification

In relation to the flight simulation model and associated analysis routines, the verification process aims to 1) verify the correctness of the numerical implementation and solution, and 2) estimate the numerical error and associated uncertainty. The second step, commonly referred to as *solution verification*, is dependent on the application or problem of interest and, thus, is the responsibility of the applicant. The

established practices outlined in, e.g., Ref. 21 do not necessarily translate directly to the multi-dimensional and multi-physics problem of rotorcraft flight simulation, particularly when it concerns solutions constrained to run in real-time where convergence criteria may need to be relaxed. A more pragmatic approach (Ref. 23) is to consider the numerical uncertainty $u_{num}$ as epistemic, i.e., an interval without associated probability distribution, where the bounds of numerical uncertainty for a given output parameter of interest are defined equal to ± the magnitude of the error relative to the *fine grid* solution.
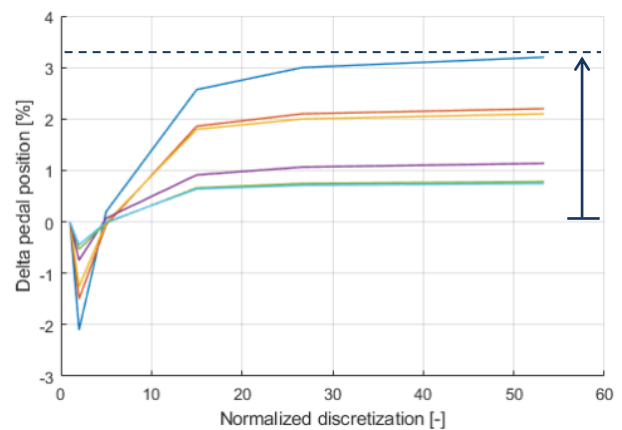


Figure 4: Discretization convergence study to establish numerical uncertainty on DoV hover-in-wind trim pedal position considering time step, number of blade aerodynamic segments, and number of inflow and interference states.

In the low-speed controllability case, the analysis may consider, e.g., the prediction of the pedal trim position or the peak yaw rate response to a pedal input. The discretisation parameters for a typical implementation may include the solution time step, the number of rotor blade aerodynamic segments, the number of inflow states, or the number or maximum age of particles in case of Vortex Particle Method analysis. Figure 4 provides an example of the convergence of the predicted hover in wind trim pedal position as a function of the such discretisation parameters, where the arrow indicates the associated numerical error. Note that for this example, the numerical uncertainty of ±3.2% is comparatively large and a refinement of the discretisation of the nominal model is desired (subject to constraints imposed for real-time piloted simulation, if applicable).

## 5.3 FSM Validation

The conventional flight simulation validation process, as stipulated, for instance in CS-FSTD(H), consists of

a comparison of the (tuned) simulation prediction against (time or frequency domain) flight test data and establishing criteria for the acceptable level of disagreement between the two. However, to support the credible extrapolation of the simulation predictions to conditions for which no flight test data are available, it is important to develop an understanding concerning the uncertainties present in both the simulation predictions and the flight test data.
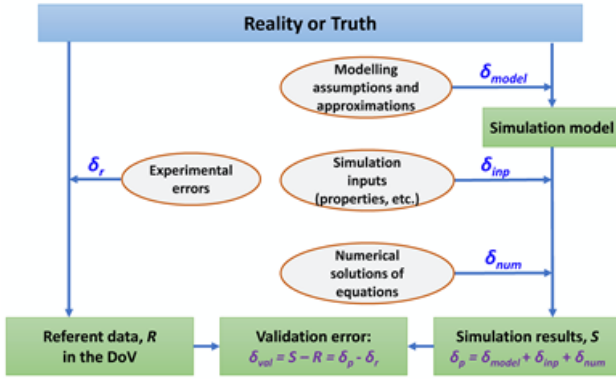


Figure 5: Representation of various errors in simulation validation against referent, adapted from Ref. 21.

Figure 5 provides an overview of the various errors and uncertainties in a typical validation exercise, adapted from Ref. 21. The reality or truth on the top of the figure is typically an unknown, even if the distinction is rarely made. The model (form) error $\delta_{model}$, that is defined in Ref. 21 as the discrepancy between the model prediction and the truth, is an uncertain parameter that lies within the range:

(1)        $\delta_{model} \in \delta_{val} \pm u_{val}$

Where $u_{val}$ is known as the validation uncertainty and $\delta_{val}$ equals the validation error. Once the range of $\delta_{model}$ has been determined from Eq. (1), the reality or truth value is estimated to lie within the interval:

(2)        $[S + \delta_{val} - ku_{val}, S + \delta_{val} + ku_{val}]$

Here, $k$ is a coverage factor that determines the confidence level (for a normal distribution, $k = 2$ represents 95% confidence). In case epistemic uncertainties are involved, which is typically the case, a coverage factor can be applied but can no longer be associated with a certain probability.

The validation error $\delta_{val}$, or the comparison error in the terminology of Ref. 21, is the difference between the simulation predictions $S$ and the measurement results $R$, both of which have uncertainty associated with them the extent of which is determined by the measurement. Under the assumption of independent

errors, the validation uncertainty $u_{val}$ is computed according to Ref. 21 as:

(3)        $u_{val} = \left( \sqrt{u_{num}^2 + u_{inp}^2 + u_R^2} \right)_{val}$

The numerical uncertainty $u_{num}$ is established in the verification phase. The input uncertainty $u_{inp}$ can be computed, e.g., through a Monte-Carlo type of analysis (depending on the types of uncertainties involved, Ref. 22) taking into account the uncertainties in the input parameters of the simulation model (for more details see section 7.1). Finally, $u_R$ is the sum of the systematic and random uncertainty in the referent data (typically test data). The latter may be defined, e.g., as the standard deviation of the flight test measurement distribution of the parameter of interest (multiplied by a coverage factor).

In the case that a Monte-Carlo analysis is performed, an estimate is obtained of the distribution of uncertainty in the model error $\delta_{model}$, from which an interval can defined in which the model error falls with a certain probability, e.g., 95% confidence (assuming purely aleatoric uncertainties). Alternative methods for estimating the model error (and the uncertainty therein) are described in, e.g, Ref. 23, which also explores the performance of the various methods in case of extrapolation from a DoV containing sparse data, considering the metrics of *conservativeness* and *tightness*. The topic of extrapolation will be revisited in section 0.

If it is found that the validation uncertainty $u_{val}$ is too large (e.g., in comparison to the proximity to the pedal limit at the intended prediction conditions), then one or more of the underlying uncertainties must be reduced. In case, after quantification of the output uncertainties, the input uncertainty is found to be the main contributor in comparison to the other sources of uncertainty, analysis of the sensitivities, or *importance factors*, can be performed to identify the dominant parameter uncertainties which should be reduced. If, instead, the validation uncertainty $u_{val}$ is small compared to the validation error $\delta_{val}$, then the model error is approximately equal to the validation error and the simulation results can, in principle, be calibrated to account for the difference (Ref. 24). In this case, care must be taken, however, when extrapolating this calibration beyond the validation domain, as will be discussed in Section 0.

Once quantified, the model error $\delta_{model}$ can be used in Phase 3 of the RCbS process to establish the total

simulation prediction error $\delta_{pred}$, or the uncertainty thereof, in conditions other than those for which validation data are available. Depending on the conditions, this will require either interpolation or extrapolation of the model error and uncertainty. The numerical and input uncertainties can be reassessed directly at the prediction conditions. Note also that the uncertainty in the model error is influenced by the measurement (referent) uncertainty $u_R$ which will carry over to the prediction conditions. This means that large measurement uncertainty in the DoV will be reflected as prediction uncertainty at the extrapolation conditions. Reductions in the uncertainty of the measurement can be achieved in various ways, including by using different instrumentation, but also by increasing the number of samples, e.g., by repeating test points or increasing the measurement period.
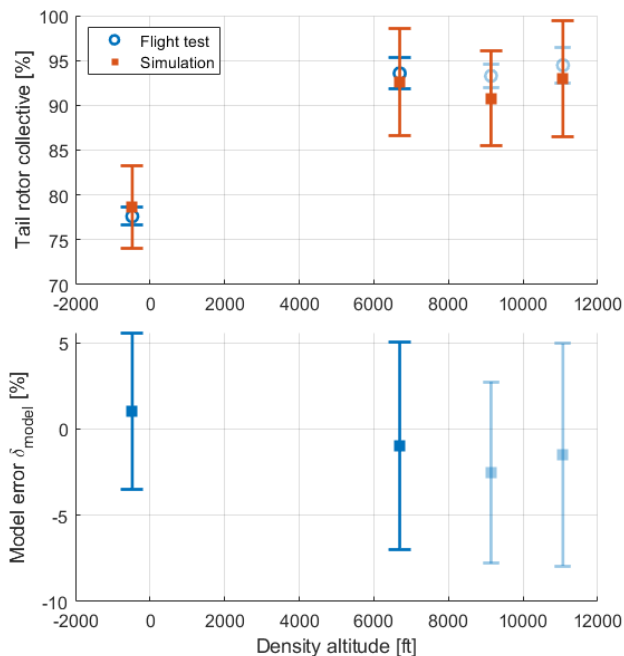


Figure 6: Validation of trim tail rotor collective prediction for OGE hover in 20±2.5 knots wind from 90±10° azimuth at maximum take-off gross weight as a function of density altitude.

Figure 6 provides an example validation exercise based on a trim assessment of the tail rotor collective position for an out-of-ground effect hover in 20±2.5 knots wind from 90±10° azimuth at maximum take-off gross weight, as a function of density altitude. The data have been obtained through certification flight test activity on the AW109 Trekker helicopter. The light blue markers indicate conditions beyond the flight test envelope (DoV) proposed for the case study and are included here for reference. The indicated

ranges for wind speed and direction reflect the differences between the test conditions, not the variation for a given trim condition. The error bars on the flight test data in the top part of the figure reflect the uncertainty in the measurement. In absence of information on the uncertainty of the instrumentation itself, only the process uncertainty associated with the test procedure is accounted for here. That is, the uncertainty in the mean computed from multiple trim recordings, as described by a Student's t-distribution (Ref. 24). The error bars around the simulation result represent the simulation total validation uncertainty $ku_{val}$ with $k = 2$ (appropriate for a situation involving only aleatory uncertainty). The bottom part of the figure plots the validation error $\delta_{val}$ (square marker), with the error bars indicating the validation uncertainty $u_{val}$ computed by Eq. (3). The model error $\delta_{model}$, by Eq. (1), must fall within the indicated range.

The input uncertainty $u_{inp}$ can be established through a Monte-Carlo analysis considering the uncertainties in the model input parameters. These uncertainties will vary between validation conditions, where much is known about the test aircraft, and predictions beyond the DoV where, e.g., operational variations of parameters across the fleet may need to be considered. To reduce the scope of the input uncertainty quantification outside of the DoV, conservative worst-case assumptions can be made for certain input parameters, such as the control rigging or minimum specification engine power, rather than specifying an interval or probability distribution. This approach is only possible in case it can truly be argued that the worst-case input parameter value leads to a worst-case result in terms of all output quantities of interest.

It can be argued based on Figure 6 that it is difficult with the test data available for this aircraft below 7,000 ft to justify a trend for extrapolation of the model error and associated uncertainty to the maximum take-off and landing altitude. In fact, besides density altitude, also the gross weight of the aircraft varies. Additional test points at intermediate altitudes, and constant referred gross weight ($GW/\sigma$), are desired to establish a credible trend and tighten the associated confidence intervals. Beyond the availability of test data, an alternative approach to the one taken in Figure 6 would be to compute (and flight test) at the 90° azimuth the wind speed that requires a trim tail rotor collective position of, say, 95%, down to a minimum wind speed of 17 knots and adjusting the take-off gross weight as needed. This would ensure a greater

consistency in the tail rotor state (at least in terms of thrust) amongst the validation conditions used to define an extrapolation to the maximum take-off and landing altitude.

Note that the process of establishing the validation uncertainty leads to a reduced emphasis on model tuning and the questionable nature thereof in terms of extrapolation. In fact, the input uncertainty $u_{num}$ should encompass the range of feasible tuning parameters. The means of the output probability distributions can then be used to characterize the fidelity of the simulation relative to the measurement through established or applicant-defined fidelity metrics, as will be discussed in the next section.

It may be tempting to forego the uncertainty quantification effort in favour of a conservative approach, in which the error relative to flight test is accepted, as long as it is conservative (even if this comes at the expense of performance). However, even with this approach it must be shown that the uncertainty of the prediction is not larger than the perceived conservativeness of the nominal FSM.

## 5.4 FSM Predictive Fidelity

Fidelity metrics are defined to provide a quantification of the level of fidelity such that criteria can be agreed on what constitutes sufficient fidelity. The key challenge is defining what is considered sufficient fidelity for a given ACR. Moreover, what may be defined as acceptable in the validation phase, may need to be reconsidered in the credibility or compliance demonstration phase based on the proximity to non-compliance with the requirements of the ACR. Where possible, it is desirable to define acceptable error tolerances, in time or frequency domains, in direct relation to the requirements of the ACR. Otherwise, it may be possible to leverage existing standards like CS-FSTD(H), if HQ and response aspects are relevant to the ACR.

Whereas the analysis to establish the validation uncertainty with the purpose of underpinning an extrapolation to compliance demonstration conditions may be limited to the primary parameters of interest (i.e., those directly related to the requirements of the ACR), the fidelity assessment must consider all relevant degrees of freedom. However, as in CS-FSTD(H), the acceptable error tolerance will vary between parameters depending on the ACR. Given the fact that this ACR revolves around controllability, the time-domain

fidelity metrics and tolerances of CS-FSTD(H) may be applied:

- Trim:
  - Control positions: ±5%
  - Pitch attitude: ±1.5°
  - Bank angle: ±2°
  - Engine torque: ±3%
- Control response (at critical azimuth):
  - Yaw rate: ±10% or ±2°/s

The tolerance of 5% on trim pedal position may be rather large for the critical azimuth where the trim margin is smallest and the applicant will want to achieve the maximum performance. An applicant may, therefore, aim for a higher accuracy from the outset for that particular trim parameter.

Frequency-domain assessments using, e.g., bandwidth and phase delay, or integrated cost functions of the magnitude and phase of the frequency response, provide a meaningful complement to time-domain analyses (Ref. 25). These frequency-domain methods are particularly suitable for application to ACRs with a handling qualities component, especially those involving small-amplitude perturbations from trim, as they are essentially linear methods. They are viewed to be less useful for the nonlinear, unsteady conditions of some ACRs. In practice, however, such test data may be difficult to obtain in the most relevant conditions, e.g., in quartering flight close to the ground.

Figure 7 shows the frequency-domain comparison between flight and the FSM for the hover pedal to yaw angle response (derived from the pedal to yaw rate response). The grayscale on the flight test data, and the 95% confidence interval, are both based on the coherence and the random error function (Ref. 26). The flight test data quality is such that the phase-limited bandwidth is undefined, but an integrated cost function of the frequency response, taking into account the coherence function, can nevertheless be obtained.

Ref. 25 proposes a guideline of $J_{ave} \leq 100$, where for a Multi-Input / Multi-Output system of $n_{TF}$ transfer functions, $J_{ave}$ is defined as:

$$(4) \quad J_{\text{ave}} = \sum_{l=1}^{n_{\text{TF}}} \left\{ \frac{20}{n_\omega} \sum_{\omega_1}^{\omega n_\omega} W_\gamma [W_g \, (|\hat{T}_c| - |T|)^2 + W_p (\angle \hat{T}_c - \angle T)^2] \right\}_l \frac{1}{n_{\text{TF}}}$$
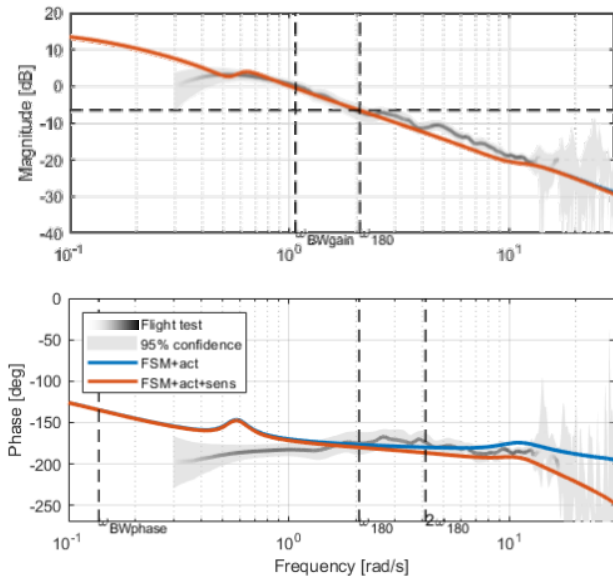
Figure 7: Out-of-ground-effect hover w/o wind pedal to yaw angle frequency response comparison between flight and simulation model.

In Eq. (4), $W_\gamma$, $W_g$ and $W_p$ are frequency ($\omega$) dependent weighting functions on coherence $\gamma$, and the magnitude $|T|$ and phase $\angle T$ of transfer function $T$. Given the weighting function conventions used in Ref. 26 and a frequency range between 0.3 and 10 rad/s, the cost function for the singular on-axis response shown in Figure 7 equals $J = 97.3$.

Finally, metrics are also required to establish the fidelity achieved in the flight simulator. For this, an applicant may propose one or more subjective rating scales such as the Simulation Fidelity Rating (SFR) described in Ref. 27, and/or the Cooper-Harper Handling Qualities Rating (HQR), Ref. 28. In either case, it will be important that the FTMs are performed and assessed consistently between flight and the simulator, preferably by the same pilots. In addition, objective metrics on, e.g., control activity or eye tracking may be included to complement and verify the subjective assessment.

## 6.  PHASE 2B: FS BUILD AND DEVELOPMENT

The RCbS process prescribes a rigorous FS build and development process following the same steps as described for the FSM. In most cases the FS is likely pre-existent, in which case documentation of past efforts may be partly relied upon assuming configuration management and record keeping are in order. Nevertheless, dedicated V&V is expected to be required. Within RoCS, the FS trials discussed herein were performed in the University of Liverpool's (UoL)

HELIFLIGHT-R simulator for the FS validation and compliance demonstration (Figure 8, Ref. 29). The simulator has a 230x70 degrees field of view, with a 4-axis force feedback control loading system and a 6 degree of freedom electric motion platform (Appendix C).



Figure 8: Cockpit view of XWH low-speed controllability ACR simulator set-up in UoL's HELIFLIGHT-R simulator (Ref. 29).

Two FTMs were explored; a pace-car equivalent (PCE) FTM, which replicates the typical flight test practice, and a cross-wind hover (XWH) FTM, which is more representative of the operational environment in which low-speed controllability issues may be encountered. The aim was, in part, to qualitatively compare the FTMs in terms of their efficacy in identifying low-speed handling quality deficiencies. Moreover, as mentioned previously, a one-to-one piloted validation requires that the evaluation is performed using the same FTM in the FS as in flight.

The XWH FTM visual references for desired (+/-2 ft) and adequate (+/-4 ft) height performance assessment were provided using blue and yellow hover boards and a red reference height ball at 45 degree intervals around the azimuth, as shown in Figure 8. Desired (+/- 3 ft) and adequate (+/- 6 ft) plan position performance references were provided by cones placed at each 45-degree azimuth. The relative wind condition could be set using the FS' Environment feature to give the required test wind velocity at any given 'visual' azimuth. For the PCE FTM, the visual database developed for a companion FTM (Ref. 30), was used, consisting of a runway with additional visual content (buildings) alongside it for height reference. The head-down flight display used in AW109 flight testing was emulated to provide information to the co-

pilot on ground speed and ground track angle for assessing the 'validity' of a test point. The EP flew the manoeuvre using outside visual references and was aided by the co-pilot in the left-hand seat calling out ground speed.

HELIFLIGHT-R's Vestibular Motion Cueing feature was tuned during the pre-trial work-up. Previous work at UoL (Refs. 31 and 32) has shown that careful selection of the parameters in the motion drive algorithms, gain and break frequency in translational and rotational axes is required to provide sufficient cueing for a given task. The values tuned for the XWH/PCE FTMs are provided in Table 2 in Appendix C.

As an example, Figure 9 shows the task performance achieved for the PCE FTM at a 30 kts, 270 degrees wind azimuth condition in the DoV (i.e., wind from 9 o'clock), which was part of an airspeed sweep starting from a hover. The FSM had already been validated against flight test data at 90 degrees wind azimuth where pedal authority was the limiting factor. However, at 270 degrees the wind speed limits are expected to be defined by handling qualities deficiencies, so the aim here was to obtain feedback from the EP on the handling qualities and the fidelity of the FS features. The green and red dashed lines in Figure 9 represent the boundaries of the desired and adequate FTM performance standards. Whilst an HQR was not awarded for this particular test point, the task performance was within desired performance for height and speed. There was an initial offset in the heading datum, but the EP could complete a heading change in this condition, in-line with the ACR, without encroaching on control limits or encountering controllability limitations. Pilot control activity is shown in Figure 10 for the 30 kts condition, which shows that no control limits are approached at this condition, and pilot compensation is minimal during the on-condition hold period. For the same azimuth, the ground speed was increased until a value of 40 kts could be achieved, again without encroaching on control limits or requiring excessive pilot compensation for handling deficiencies (to re-iterate: this condition was not formally evaluated via the award of an HQR).

At 42 kts the task was abandoned as it was not possible to maintain FTM performance parameters in height and heading. The EP reported strong side force cues due to yaw, and heave due to sideslip velocity couplings and commented that neither of these phenomena were expected dynamics of the Trekker. The two deficiencies made heading control and

height control difficult at high wind speeds, and created a handling qualities limit, as may be expected at this wind azimuth.
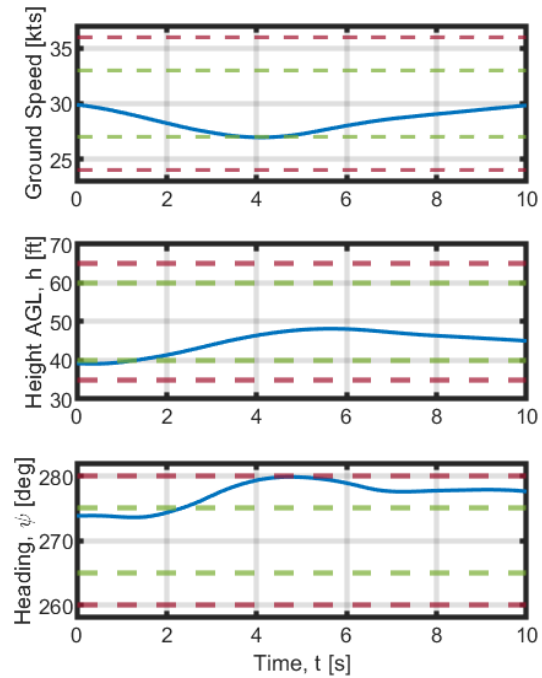


Figure 9: PCE FTM task performance for 30 kts, 270 degrees wind azimuth within DoV.
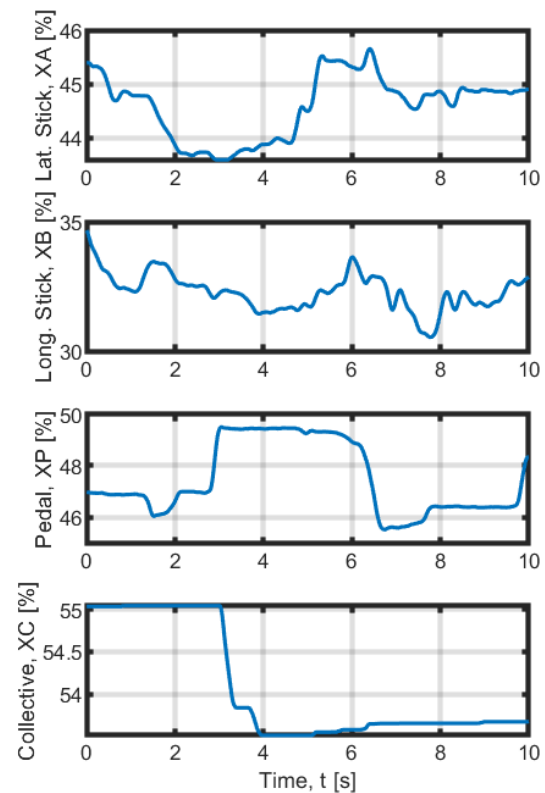


Figure 10: PCE FTM EP Control Activity for 30 kts, 270 degrees wind azimuth, within DoV.

Note that, although the FS testing served its purpose in terms of exercising the RCbS process and exploring the FS set-up, it may be clear for those that are familiar with helicopter low-speed controllability testing, or the AW109 Trekker in particular, that a wind speed of 40 kts at a relative direction of 270 degrees is excessive. In fact, the FSM employed here is not able to reproduce the handling qualities limitations experienced on the real aircraft in the azimuth range between 180 deg and 270 deg, related to the fidelity deficiencies in the main rotor wake/tail rotor interactions and tail rotor VRS.

# 7. PHASE 3: CREDIBILITY ASSESSMENT & COMPLIANCE DEMONSTRATION

## 7.1 FSM Credibility Assessment

Ultimately, it is the task of the applicant to convince the certification authority that the simulation results are credible. In the absence of test data at the certification conditions, it is impossible to provide mathematical proof, but efforts can be made to quantify the confidence in the predictions. Beyond the mathematically quantifiable, there are other factors that influence the credibility, such as the expertise and experience of the engineers involved and the rigour applied to the simulation development and its application as a whole. The following discussion will be limited to the uncertainty quantification of the prediction in the DoE as it relates to the FSM.

Prior to going into details regarding uncertainty quantification in the DoE, it is worthwhile to first elaborate on the types of uncertainty that must be accounted for, namely aleatory and epistemic uncertainty. Aleatory uncertainty is irreducible uncertainty due to inherent variation and is characterised by a probability distribution. Epistemic uncertainty is the result of a lack of knowledge and is represented by an interval or *degree of belief* distributions, or other bounding methods. Typically, both types of uncertainty exist, resulting in interval-valued (imprecise) output probability distributions such as shown in Figure 11, taken from Ref. 19. In line with the discussion in section 5.3, the sources of uncertainty in the DoE include numerical approximation uncertainty, model input uncertainty, and model form uncertainty. The numerical uncertainty can typically be considered epistemic, i.e., as an interval. The model form uncertainty, which is also epistemic, is identified in the validation phase as $u_{val}$ and must be extrapolated to the prediction conditions in the DoE. The derivation of the model input uncertainty follows the same process as in Phase 2a,

except that the analysis is now performed in the DoE. In most cases, the input and model form uncertainties will be of mixed nature. In the end, the result can be reduced to an interval within which the truth is estimated to lie with a certain confidence, e.g., through the methods explored in Refs. 21-24.
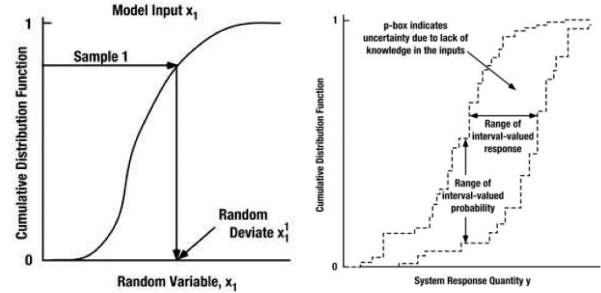


Figure 11: Notional probability distributions for pure aleatory uncertainty (left) and mixed aleatory-epistemic uncertainty (right).

The model form uncertainty in the DoV was computed in Phase 2a as the validation uncertainty:

$$(5) \qquad u_{model,val} = \left( \sqrt{u_{num}^2 + u_{inp}^2 + u_R^2} \right)_{val}$$

The prediction uncertainty in the DoE, $u_{pred}$, then becomes:

$$(6) \qquad u_{pred} = \left( \sqrt{u_{num}^2 + u_{input}^2 + u_{model}^2} \right)_{pred}$$

The model form uncertainty at the prediction condition $u_{model,pred}$ must be obtained through extrapolation of $u_{model,val}$. In the current example, $\delta_{val}$ is of similar order of magnitude as $u_{val}$, as evident from Figure 6. The prediction error at the extrapolated condition can be defined by:

$$(7) \qquad \delta_{pred} \in \delta_{val,pred} \pm u_{pred}$$

Here, both $u_{pred}$ and $\delta_{val,pred}$ are obtained, at least in part, through extrapolation. Figure 12 presents the result of an extrapolation of the model error and uncertainty into the DoE. In this case, advantage has been taken of data available in what, for the purpose of this example, is considered the DoE (>7,000 ft density altitude) in order to have sufficient data points to establish a trend from which confidence bounds can be estimated. Conservatively, the model form uncertainty and the validation error at 12,000 ft equal 4.1% and 0.3% of the total pedal travel, respectively. The conservative range for the validation error is on the negative side since it will be applied as a correction to the simulation prediction. Note, that the extrapolation in

Figure 12 is one-dimensional in density altitude, whereas a multi-dimensional regression fit would be more appropriate.
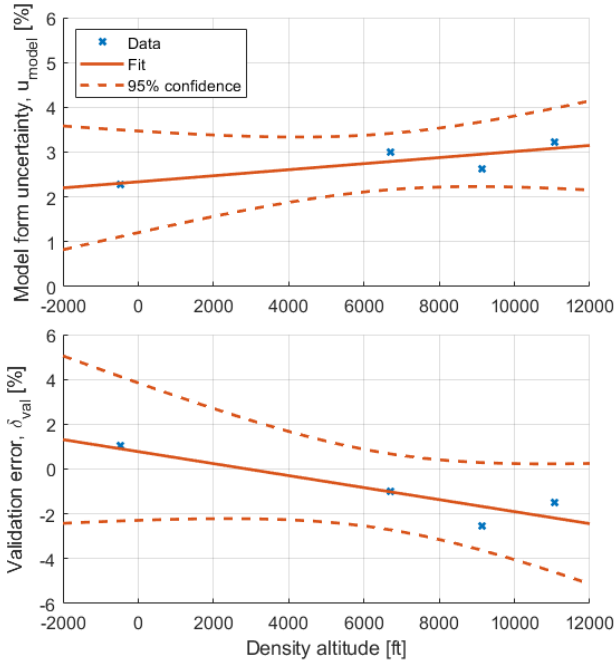


Figure 12: Linear regression fit of simulation model form uncertainty and validation error, including 95% confidence bounds, for an OGE hover in 20±2.5 kts wind from 90±10°.

Figure 13 presents the resulting trim pedal margin prediction in the DoE where the simulation prediction at 12,000 ft density altitude has been calibrated (or corrected) by the extrapolated validation error, and uncertainty bounds added to account for extrapolated model form uncertainty, as well as the input and numerical uncertainties at the prediction conditions. The question as to whether or not this result is acceptable from a compliance perspective will depend on the control margin required to achieve the requisite noticeable yaw rate, but it is clear from Figure 13 that the uncertainty around the simulation reduces the performance margin.

The analysis described thus far has been limited to an offline trim pedal margin assessment with wind from the critical azimuth (90 degrees). Typically, there are also wind speed limitations related to handling qualities. For the AW109 Trekker, the wind envelope is limited by handling qualities at a relative wind direction between 160 and 260°. The simulation-based compliance demonstration for such limitations requires piloted simulation in a suitable FS, as will be discussed in the following section.
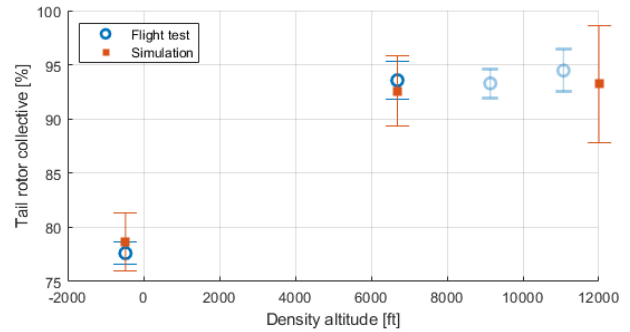


Figure 13: Extrapolation of trim tail rotor collective up to 12,000 ft density altitude, for an OGE hover in 20±2.5 kts wind from 90±10°.

## 7.2 DoE FS Testing

This section contains preliminary results from piloted simulations at UoL in which an EASA pilot, amongst other test pilots, flew a mock certification compliance demonstration simulation trial for the low-speed controllability ACR.

The FSM used for the piloted trials corresponded to the configuration described in Section 5.1 without further modification or variation. A more rigorous approach would involve a similar FSM uncertainty quantification exercise as described above, but with a focus on relevant objective handling qualities metrics. In this way, the FS trials could be set up to reflect a FSM configuration that falls on the conservative side of the uncertain range of predicted handling qualities.

### 7.2.1 FTM Comparison

The compliance demonstration phase of the FS trials was performed using the XWH FTM, but the flight condition was also assessed using the PCE FTM to facilitate comparison of the two methodologies. Figure 14 shows the task performance over the 10 seconds 'stabilised' phase, for both FTMs for a 30 kts, 240 degree wind azimuth case within the DoE. Note that the green and red dashed lines again represent the performance standards, but in plot (b) the dashed red line indicates adequate performance for the XWH FTM, and the dotted red line indicates the adequate performance standard for the PCE FTM.

In the XWH FTM, the EP reported there was "beyond extensive" pilot compensation to capture the required wind azimuth angle and once 'on condition' there was considerable to extensive pilot compensation required to achieve adequate task performance. It is noted that the compensation required to capture the desired heading is not accounted for in the award of
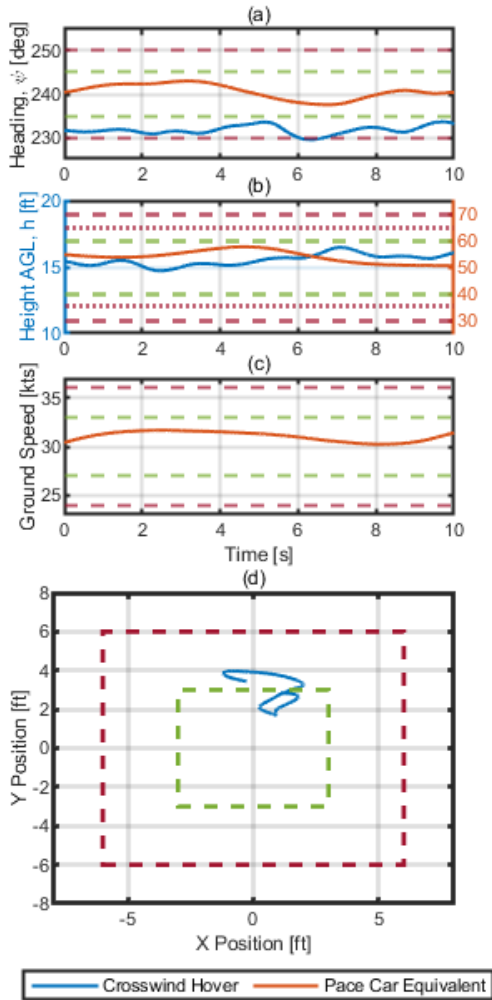
Figure 14: XWH and PCE FTM performance for 30 kts wind at 240 degrees azimuth in the DoE.

an HQR for the FTM, but it did provide insight into the handling qualities deficiencies of the simulated aircraft, primarily due to the side force cues due to yaw also identified in the PCE FTM. Pilot control activity for the two manoeuvres is shown in Figure 15. Plan position was 'adequate' and there was a heading bias that resulted in adequate performance in heading, which the pilot commented was due to a high angle of bank in the trim condition. Conversely, in the PCE, both the heading and ground speed remained within desired performance bounds throughout the required 10 second on-condition hold period.

The pilot control activity in Figure 15 shows oscillatory inputs in all 4 control axes for the XWH manoeuvre, which are not present in the PCE, where pilot compensation was considerable. These oscillatory inputs appear to be driven by higher piloting gains that are forced by the performance standards of the XWH which, relative to the PCE, are tighter; a 3 kt

groundspeed (desired performance in the PCE) would take the pilot out of desired performance in the XWH FTM in approximately 0.6 seconds, which a pilot would struggle to respond to quickly enough to correct for. As a result, the pilot had to apply larger corrective inputs to maintain the given performance standards.
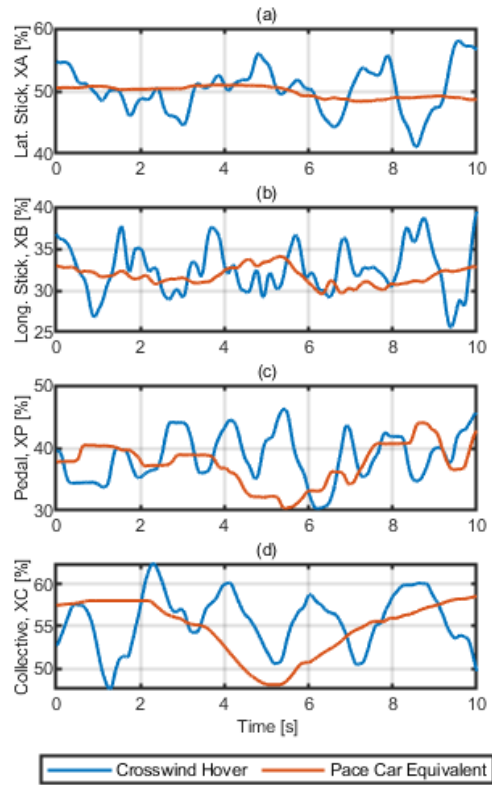


Figure 15: XWH and PCE EP Control Activity for 30 kts wind at 240 degrees azimuth in the DoE.

Generally, the perceived handling qualities in the XWH and PCE FTMs were not equivalent even though the physics of the simulated aerodynamics are theoretically identical. The different piloting strategies highlighted different deficiencies in the FSM, the FS and the perceived handling qualities. The XWH FTM, with the associated performance targets specified, was characterised by higher piloting gains. The disparities between the two FTMs highlight a scenario where performance may be degraded and result in a lower HQR (if an HQR methodology is adopted) in a more representative task than the existing compliance demonstration methodology.

### 7.2.2 FSM Variations

In both FTMs, the EP reported the strong side force cues due to yaw, and heave due to sideslip velocity couplings, and both made aspects of each task more difficult, particularly height maintenance in the PCE,

and heading capture in the XWH. It was theorised that this may be a result of unpredicted interactions with the fuselage interference model, and a short experiment was conducted to compare the behaviour of the FSM with fuselage interference enabled (the option used in the testing described so far) and disabled. The testing was performed using the XWH FTM in a 10 kts wind at 240 degrees azimuth.
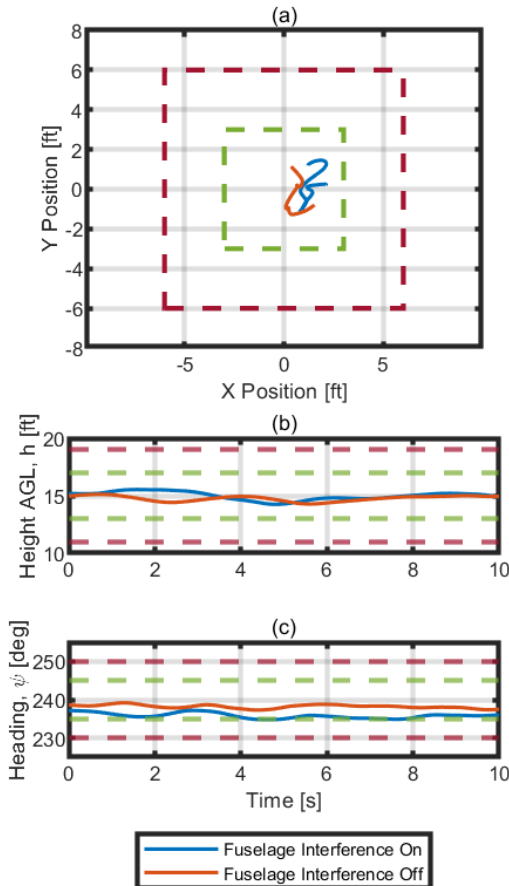


Figure 16: XWH FTM Performance for 10 kts wind at 240 degrees azimuth in the DoE, with FSM fuselage interference turned ON and OFF.

A comparison of the task performance of the two FSM variants is shown in Figure 16. In both cases, the pilot is able to maintain desired performance at this low wind speed, but heading performance for the fuselage interference ON case is borderline, and the pilot reported moderate compensation in all axes and awarded an HQR 4. The pilot control activity for the XWH FTM with the two FSM variants is shown in Figure 17. With fuselage interference turned OFF, the pilot reported reduced compensation in cyclic, and awarded an HQR 3, indicating only minimal compensation required for desired performance. The effect of

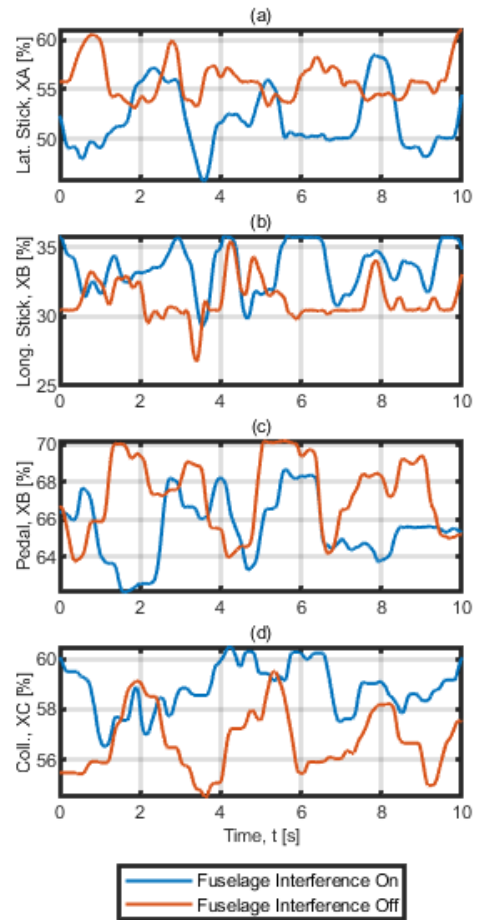this FSM variation will be further investigated to fully quantify its effect on model fidelity.



Figure 17: XWH FTM pilot control activity for 10 kts wind at 240 degrees azimuth in the DoE, with FSM fuselage interference turned ON and OFF.

### 7.2.3 Effect of Vestibular Motion Cueing

Limited time was available for examination of the Vestibular Motion Cueing FS feature for this ACR. For the PCE FTM, a motion fidelity rating of 4 was awarded, whereas for the XWH FTM a motion fidelity rating of 6 was awarded indicating that, for both FTMs, vestibular motion was useful in the FTM, but for the XWH FTM, some annoying deficiencies were present and other cues were more dominant. Further testing is required to aid in the optimisation of this FS feature going forward.

## 8. CONCLUDING REMARKS AND RECOMMENDATIONS

This paper has reported on an exercise of the RCbS process and presented results from the case study on

the low-speed controllability ACR as expressed in CS-27 and 29.

Conclusions from the case study are as follows:

(i). The FSM model employed in this study is not able to reproduce the low-speed handling quality deficiencies of the real aircraft; advances in the state of the art are required for this ACR to be addressed fully through simulation.

(ii). Nevertheless, the case study provided a useful basis for exploring the practical implementation of the RCbS process and its associated benefits and limitations. FSM V&V and credibility assessment efforts focused on the prediction of the trim pedal margin limit for which the current FSM is more suitable.

(iii). The uncertainty-centric approach taken in the RCbS V&V and credibility assessment phases puts a new perspective on FSM fidelity and model updating, especially in areas of the flight envelope where no test data is available (the DoE).

(iv). Using a FSM outside of its DoV inherently introduces uncertainty. The quantification of this uncertainty is one of the key elements of the simulation credibility assessment. The prediction uncertainty unavoidably comes at the expense of performance margin.

(v). Careful deliberation is required to decide which certification requirements may feasibly be tackled using simulation in a manner that is cost-effective and does not unduly compromise certified performance.

(vi). To support RCbS, development and certification flight test activities must be set-up with utility for FSM and FS validation in mind. This includes flight test instrumentation and general documentation considerations, as well as judicial test point selection anticipating extrapolation requirements.

(vii). The XWH and PCE FTMs do not produce equivalent HQ ratings, highlighting different deficiencies and displaying differences in piloting gains.

The paper is one of a collection of case studies presented at the 49th ERF, material from which will be included in the final issue of the RoCS project Guidelines for the application of modelling and simulation in rotorcraft certification, scheduled for publication in late 2023.

Author contacts:

| | |
|---|---|
| Stefan van 't Hoff | stefan.van.t.hoff@nlr.nl |
| Mark White | mark.white@liverpool.ac.uk |
| Chris Dadswell | sgcdadsw@liverpool.ac.uk |
| Linghai Lu | l.lu@cranfield.ac.uk |
| Gareth Padfield | gareth.padfield@liverpool.ac.uk |
| Giuseppe Quaranta | giuseppe.quaranta@polimi.it |
| Philipp Podzus | philip.podzus@dlr.de |

## 9. ACKNOWLEDGMENTS

## 10. REFERENCES

1. R. Bianco-Mengotti, A. Ragazzi, F. Del Grande, G. Cito e A., and Brusa Zappellini, "AW189 Engine-Off-Landing Certification by Simulation," AHS 72nd Annual Forum, West Palm Beach, FL, May 17-19, 2016.

2. A. Ragazzi, R. Bianco-Mengotti, and P. Sabato, "AW169 Loss of Tail Rotor Effectiveness Simulation," 43rd European Rotorcraft Forum, Milano, Italy, September 12 – 15, 2017.

3. Anon., "Certification Specifications and Acceptable Means of Compliance for Small Rotorcraft CS-27 / Amendment 6," EASA, 2018.

4. Anon., "Certification Specifications and Acceptable Means of Compliance for Large Rotorcraft CS-29 / Amendment 5," EASA, 2018.

5. Anon., "AC 29-2C - Certification of Transport Category Rotorcraft," FAA, Sept. 2008.

6. Anon., "AC 25-7D Flight Test Guide for Certification of Transport Category Airplanes," FAA, 2018.

7. G. D. Padfield, "Rotorcraft Virtual Engineering; Supporting Life-Cycle Engineering through Design and Development, Test and Certification and Operations," The Aeronautical Journal, Vol. 122, No. 1255, pp. 1475–1495, 2018.

8. G. Quaranta, S. van 't Hoff, M. Jones, L. Lu, and M. D. White, "Challenges and Opportunities Offered by Flight Certification of Rotorcraft by Simulation," 47th European Rotorcraft Forum, Glasgow, Scotland, UK September 7-9, 2021.

9. Van 't Hoff S, Lu L., Padfield G., Podzus P., White M., and Quaranta G., "Preliminary Guidelines for a Requirements-Based Approach to Certification by Simulation for Rotorcraft", 48th European Rotorcraft Forum, Winterthur, September 6-8, 2022.

10. G. Quaranta, S. van 't Hoff S, L. Lu, G.D. Padfield, P. Podzus, M. White, "Employment of Simulation for the Flight Certification of Rotorcraft", 49th Annual Forum of the Vertical Flight Society, West Palm Beach, FL, USA, May 16-18, 2023.

11. https://www.rocs-project.org/guidelines/ accessed 28th July 2023.

12. C. He, C.S. Lee, and W. Chen, "Finite State Induced Flow Model in Vortex Ring State", American Helicopter Society 55th Annual Forum, Montreal, Canada, May, 1999.

13. W. Johnson, "Model for Vortex Ring State Influence on Rotorcraft Flight Dynamics", NASA/TP-2005-213477, December, 2005.

14. D.A. Peters, C. He., "Modification of Mass-Flow Parameter to Allow Smooth Transition Between Helicopter and Windmill States", Journal of the American Helicopter Society, July, 2006,Vol. 51, No. 3, pp. 275-278.

15. Anon., ADS-33E, "Aeronautical Design Standard Performance Specification: Handling Qualities Requirements for Military Rotorcraft," US Army Aviation Engineering Directorate, Redstone, Alabama, March 2000.

16. M. White, C. Dadswell, G. Padfield, S. van 't Hoff, R. Bakker, L. Lu, Q. Quaranta and P. Podzus, "Case Studies to Illustrate the Rotorcraft Certification by Simulation Process: CS 29/27 Category A Rejected Take-off, Confined Area", 49th European Rotorcraft Forum, Bückeburg, Germany, September, 2023.

17. Anon., "Certification Specifications for Helicopter Flight Simulation Training Devices CS-FSTD(H)", EASA, Initial issue, June 2012.

18. DuVal, R.W., and HE, C., "Validation of the FLIGHTLAB Virtual Engineering Toolset", The Aeronautical Journal, 2018, 122, (1250), pp. 519-555.

19. C. He, M. Syal, M.B. Tischler and O. Juhasz, "State-Space Inflow Model Identification from Viscous Vortex Particle Method for Advanced Rotorcraft Configurations", American helicopter Society 73rd Annual Forum, Fort Worth, Texas, USA, May, 2017.

20. C. He and J. Zhao, "A Real Time Finite State Induced Flow Model Augmented with High Fidelity Viscous Vortex Particle Simulation", American Helicopter Society 64th Annual Forum, Montreal, Canada, April, 2008.

21. Anon., "Standard for verification and Validation in Computational Fluid Dynamics and heat Transfer", ASME V&V 20-2009.

22. I. Ioannou, P.O. Hristov, H.K. Yong, R. Marsh, E. Silva, A. Sobester and S. Ferson, "Towards a Framework for Non-instrusive Uncertainty Propagation in the Preliminary Design of Aircraft System, AIAA 2023-2373, AIAA SciTech Forum, National Harbor, Maryland, 2023.

23. C.J. Roy and W.L. Oberkampf, "A Complete Framework for Verification, Validation, and Uncertainty Quantification in Scientific Computing", 48th AIAA Aerospace Sciences Meeting, Orlando, Florida, USA, January, 2010.

24. N.W. Whiting, C.J. Roy, E. Duque, S. Lawrence, and W.L. Oberkampf, "Assessment of Model Validation, Calibration, and Prediction Approaches in the Presence of Uncertainty", ASME, Journal of Verification, Validation and Uncertainty Quantification, Vol. 8, Issue 1, March, 2023.

25. M. Pavel, M. Tischler, M. White, O. Stroosma, M. Jones, D. Miller, V. Myrand-Lapierre, M. Nadeau-Beaulieu, A. Taghizad, "Simulation Fidelity Assessment for Rotorcraft Methods and Metrics Sketches from the Work of NATO AVT-296", 77th Annual Vertical Flight Society Forum, Virtual, United States, May, 2021.

26. M.B. Tischler and R.K. Remple, "Aircraft and Rotorcraft System Identification: Engineering Methods with Flight Test Examples", AIAA, August, 2006.

27. Perfect P, Timson E, White MD, Padfield GD, Erdos R and Gubbels AW, "A Rating Scale for the Subjective Assessment of Simulation Fidelity", The Aeronautical Journal, August, Volume 11, No 1206, pp. 953 – 974, 2014.
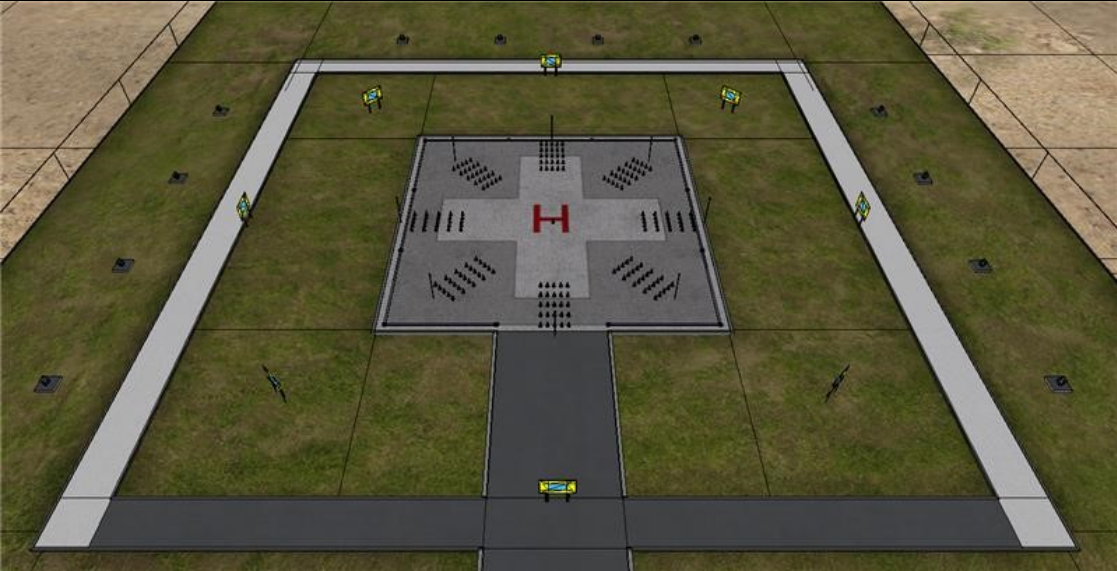
28. G. E. Cooper and R. P. Harper, "The Use of Pilot Ratings in the Evaluation of Aircraft Handling Qualities, NASA TN D-5153," NASA, 1969.

29. M.D. White, P. Perfect, G.D. Padfield, A.W. Gubbels and A.C. Berryman, "Acceptance testing and commissioning of a flight simulator for rotorcraft simulation fidelity research" in Proceedings of the Institution of Mechanical Engineers, Part G: Journal of Aerospace Engineering, Volume 227 Is-sue 4, pp. 663 – 686, April 2013

30. L. Lu, G.D. Padfield, M.D. White, G. Quaranta, S. van 't Hoff, and P. Podzus, "Case Studies to Illustrate the Rotorcraft Certification by Simulation Process; CS 29/27 Dynamic Stability Requirements", submitted to 49th European Rotorcraft Forum, Bückeberg, Germany, 5–7th September 2023.

31. S.J. Hodge, P. Perfect, G.D. Padfield, and M.D. White, "Optimising the Yaw Motion Cues Available from a Short Stroke Hexapod Motion Platform", The Aeronautical Journal, January, 2015, Vol. 119, No. 1211, pp. 1-21.

32. S.J. Hodge, P. Perfect, G.D. Padfield, and M.D. White, "Optimising the Roll-Sway Motion Cues Available from a Short Stroke Hexapod Motion Platform", The Aeronautical Journal, January, 2015, Vol. 119, No. 1211, pp. 23-44.

## APPENDIX A: PACE-CAR EQUIVALENT (PCE) FTM DESCRIPTION

| Mission | Civil Transport |
|---|---|
| **Critical HQs** | Yaw attitude quickness and bandwidth<br>Lateral-directional stability<br>Pitch & Roll bandwidth<br>Cross-couplings: pitch/roll, roll/pitch, collective/yaw, collective/pitch |
| **Objectives** | • Assess handling qualities in 'hover' under crosswind conditions<br>• Check ability to perform heading transitions in crosswind conditions<br>• Assess the effect of vestibular motion cueing on pilot perception of simulation fidelity |
| **Manoeuvre Description** | The FTM begins with the aircraft in a stabilised hover, 50ft AGL, at one end of the runway on a heading of $\psi_W$, over the runway centreline. The EP will initiate a transition along the centreline of the runway, accelerating to a ground speed of $V_W$. Once the aircraft has reached $V_W$, the EP must maintain ground speed, heading and altitude within specified performance standards, for a period of 10 seconds. A 10s timer can be initiated by pressing the cyclic grip trigger button; the EP must not initiate the timer before reaching $V_W$. The EP will be cued once 10 seconds has elapsed, the EP must adjust heading to exceed $\psi_W + 5°$ whilst maintaining runway centreline, altitude, and ground speed, and then adjust heading to exceed $\psi_W - 5°$, again maintaining other performance standards. The task is complete once the EP has attained $\psi_W \pm 5°$ following heading hold. |
| **Test Course Description** | Standard runway in an open area. Testing will be conducted in VMC. |

| Test Variations | Condition | Mass | Pressure Altitude |
|---|---|---|---|
| | | 3,115kg<br><br>Increments up to MTOW kg | 745ft<br><br>10,000ft |

| Ratings Scales | 1. Cooper-Harper Handling Qualities Rating Scale (Ref. 28)<br>2. Simulation Fidelity Rating Scale (Ref. 27) | | |
|---|---|---|---|

| Performance Standards | | Desired (*d*) | Adequate (*a*) |
|---|---|---|---|
| | Maintain ground speed, $\delta V_W$: | ±3 kts | ±6 kts |
| | Maintain altitude $\delta h$: | ±10 ft | ±15 ft |
| | Maintain heading $\delta \psi_W$ : | ± 5º | ± 10º |

GENESYS

White line 'driven' by model output of groundspeed and ground track angle. White circles at 10,20 knots

## APPENDIX B: CROSS-WIND HOVER (XWH) FTM DESCRIPTION

| Mission | Civil Transport |
|---|---|
| **Critical HQs** | Yaw attitude quickness and bandwidth<br>Lateral-directional stability<br>Pitch & Roll bandwidth<br>Cross-couplings: pitch/roll, roll/pitch, collective/yaw, collective/pitch |
| **Objectives** | • Check ability to perform precise hover control<br>• Check ability to perform heading transitions from hover to hover in wind conditions<br>• Assess effect of vestibular motion cueing on pilot perception of simulation fidelity<br>• Assess sufficiency of visual cueing for the task |
| **Manoeuvre Description** | The EP will be released trimmed in a hover above the helipad, at a skid height of 10ft, on a nominal heading 45degrees from the critical azimuth. The EP will be expected to perform a 45-degree left-hand turn onto the critical azimuth and maintain a 10s hover once stabilised. The EP will press the cyclic grip trigger button to indicate they have achieved a stabilised hover at the new heading; this initiates an audio cue for the start and end of the 10s timer. Following this, the EP will attempt +5degrees and -5degrees heading change from the critical azimuth while maintaining plan position and hover height. Performance standards will not be assessed during the initial azimuth capture, but EP commentary for the transition phase will be recorded. |
| **Test Course Description** | Helipad surrounded by hover boards indicating lateral position and height performance standards on each heading. Cones will also be provided to indicate longitudinal position performance bounds for each hoverboard. Testing will be conducted in VMC. |

| **Test Variations** | **Condition** | **Mass** | **Pressure Altitude** |
|---|---|---|---|
| | | 3115kg<br>Increments up to<br>MTOW kg | 745ft<br>10000ft |

| **Ratings Scales (Max. 2 per Test Point)** | 1. Cooper-Harper Handling Qualities Rating Scale (Ref. 28)<br>2. Simulation Fidelity Rating Scale (Ref. 27) | | |
|---|---|---|---|

| **Performance Standards** | | **Desired (*d*)** | **Adequate (*a*)** |
|---|---|---|---|
| | Maintain lateral/longitudinal position: | ±3 ft | ±6ft |
| | Maintain hover height $\delta h$: | ±2 ft | ±4 ft |
| | Maintain heading $\delta \psi$: | ± 5º | ± 10º |

**APPENDIX C: HELIFLIGHT-F SIMULATOR SPECIFICTIONS**
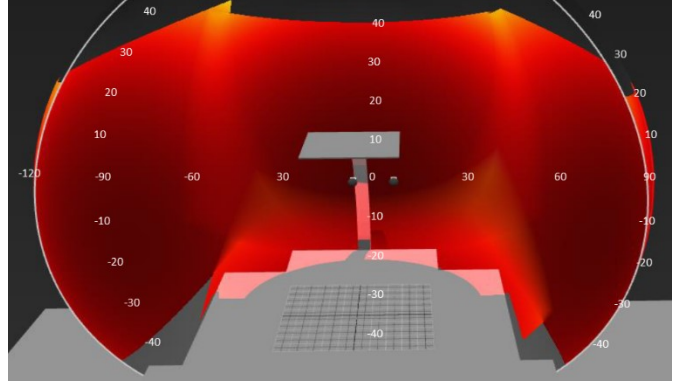


(a)                                                                    (b)

Figure C1: Liverpool's HELIFLIGHT-R research simulator (a) (Ref. 29) and projector FoV (b), coloured areas indicating dome image brightness coverage (deeper red represents higher brightness).

Table C1: HELIFLIGHT-R motion capability.

|        | Displacement   | Velocity  | Acceleration |
|--------|----------------|-----------|--------------|
| Pitch  | -23.3°/+25.6°  | ±34°/s    | >300°/s²     |
| Roll   | ±23.2°         | ±35°/s    | >300°/s²     |
| Yaw    | ±24.3°         | ±36°/s    | >500°/s²     |
| Heave  | ±0.39m         | ±0.7m/s   | ±1.02 g      |
| Surge  | -0.46m/+0.57m  | ±0.7m/s   | ±0.71g       |
| Sway   | ±0.47m         | ±0.5m/s   | ±0.71g       |

Simulator platform movements are determined by the MDA that scale, limit and filter the signals from the FSM to generate VeMCS commands. An example of a third-order filter used for the pitch axis MDA is given in Eqn. (C1) which scales and filters the FSM yaw acceleration, $\ddot{\psi}$, converting it into a commanded motion platform yaw acceleration, $\ddot{\psi}_s$. The parameters $k_\psi$ and $\omega_{hp\psi}$ are the yaw high pass (hp) filter gain and break-frequency coefficients, respectively which are 'tuned' for a given FTM. Similar filters are used in other rotational ($\phi$, $\theta$) and the translational axes (*x*, *y*, *z*).

(C1)     $\dfrac{\ddot{\psi}_s}{\ddot{\psi}}(s) = k_\psi HP_\psi(s) = k_\psi \left(\dfrac{s^2}{s^2 + 2\zeta_{hp\psi}\omega_{hp\psi}s + \omega_{hp\theta}^2}\right)\left(\dfrac{s}{s+\omega_{b\psi}}\right)$

Table C2: XWH and PCE FTM MDA parameters

| MDA | Surge | | Sway | | Heave | | Roll | | Pitch | | Yaw | |
|---|---|---|---|---|---|---|---|---|---|---|---|---|
| | $k_x$ | $\omega_{hpx}$ | $k_y$ | $\omega_{hpy}$ | $k_z$ | $\omega_{hpz}$ | $k_\phi$ | $\omega_{hp\phi}$ | $k_\theta$ | $\omega_{hp\theta}$ | $k_\psi$ | $\omega_{hp\psi}$ |
| XWH & PCE | 0.5 | 1 | 0.4 | 1 | 0.55 | 3 | 0.28 | 0.4 | 0.2 | 0.4 | 0.6 | 0.4 |